RSC Advances

PAPER

View Article Online
View Journal | View Issue

Cite this: *RSC Adv.*, 2017, **7**, 51090

Mesoporous $Ag_1(NH_4)_2PW_{12}O_{40}$ heteropolyacids as effective catalysts for the esterification of oleic acid to biodiesel†

Qiu-yun Zhang, *[abc] Fang-fang Wei,[ac] Qian Li,[a] Jin-shu Huang,[a] Yun-mei Feng[a] and Yu-tao Zhang[a]

Received 23rd September 2017
Accepted 21st October 2017

DOI: 10.1039/c7ra10554a

rsc.li/rsc-advances

Mesoporous $Ag_1(NH_4)_2PW_{12}O_{40}$ (AgN-PW) was developed by co-doping silver and ammonium ions into phosphotungstic acid as an efficient and stable catalyst for free fatty acid esterification, and its physicochemical properties were derived from X-ray diffraction (XRD), thermogravimetric (TG) analysis, Fourier transform infrared (FT-IR) spectra, N_2 adsorption–desorption, scanning electron microscopy (SEM) and transmission electron microscopy (TEM). The final catalyst showed a typical Keggin structure of heteropoly acids. This solid acid exhibited remarkable catalytic activity (nearly 100% conversion) in the esterification of oleic acid with methanol for biodiesel production under optimum synthesis conditions. Furthermore, due to the high activity presented in various esterifications of free fatty acids and non-edible oils with high acid values, the mesoporous AgN-PW material was proven to be an environmentally friendly catalyst for industrial biodiesel production.

1. Introduction

The perpetual demand for fuels worldwide has increased tremendously which partly relies on fossil fuels. However, carbon emissions from fossil fuel burning have also increased which causes global warming. Focusing on this aspect, renewable and clean energy sources are currently in high demand.[1–3] Biodiesel has attracted much attention in recent years as an alternative renewable and sustainable energy source which is easy to handle, is nontoxic, carbon-neutral and biodegradable.[4] Biodiesel (a fatty acid alkyl ester) is basically produced from free-fatty acids (FFAs), edible oils or animal oils by esterification or transesterification with short-chain alcohols using acid or base catalysts.[5] However, one of the big challenges is the high-cost feedstocks of edible vegetable oils and animal oils.[6] Therefore, it is necessary to seek inexpensive non-edible oil sources containing high concentrations of FFAs, *e.g. Euphorbia lathyris* oil,[7] *Madhuca indica* oil,[8] *Camelina sativa* oil[9] or waste cooking oils.[10] On the other hand, base catalysts are not recommended for the production of biodiesel due to potential saponification.[11] Therefore, the acid-catalyzed esterification of FFAs is a safer choice.

Although homogeneous acids such as H_3PO_4, HCl and H_2SO_4 are relatively cheap, are available and have high catalytic activity, they are usually difficult to separate and purify from products and are corrosive to equipment, leading to an increase in biodiesel production costs and to environmental problems.[12] To overcome these drawbacks, different types of solid acid catalyst are used with excellent reusability, convenient product separation, low corrosion, water tolerance and environmental compatibility, offering good potential for the substitution of homogeneous acids. Recently, several solid acid catalysts have been employed in the esterification of FFAs with methanol for biodiesel production, such as picolinic acid-modified 12-tungstophosphoric acid,[13] HMCM-36 zeolite,[14] Pr-SO_3H-functionalized SBA-15,[15] sulfated zirconia,[16] metal-modified graphene oxide composite catalysts,[17] *etc.*

Heteropoly acids are a kind of environmentally friendly material and possess strong Brønsted acidity, and are used as acid catalysts for dehydration, etherification, esterification and transesterification.[13] Moreover, the acid sites of heteropoly acids are more uniform and easier to control than those of other acid catalysts. However, the recovery of heteropoly acids is difficult and complicated, because of their small particle size or their solubility in polar solvents. Recently, the partial substitution of H^+ in phosphotungstic acid (HPW) with large monovalent ions such as Cs^+, Ag^+, K^+ and NH_4^+ has been considered as an effective technique to create major changes in its pore structure to improve the surface area and solubility of the pristine acids.[18,19] Narasimharao *et al.*[20] found that

[a]*School of Chemistry and Chemical Engineering, Anshun University, Anshun 561000, Guizhou, China. E-mail: sci_qyzhang@126.com*

[b]*Guizhou University, Guiyang 550025, Guizhou, China*

[c]*Engineering Technology Center of Control and Remediation of Soil Contamination of Provincial Science & Technology Bureau, Anshun, Guizhou, 561000, China. E-mail: weiff@iccas.ac.cn*

† Electronic supplementary information (ESI) available: Reusability study of the catalyst, FT-IR spectra of the fresh AgN-PW catalyst and the reused catalyst, and catalytic performance of AgN-PW for other esterification reactions. See DOI: 10.1039/c7ra10554a

$Cs_xH_{3-x}PW_{12}O_{40}$ salts were active for the esterification of palmitic acid. Santos *et al.*[21] reported a novel mixed salt of cesium and ammonium derivatives of H_3PW with good catalytic activity. However, there are presently no reports available of other cation co-doped heteropoly acids for the esterification of FFAs with methanol for the production of biodiesel.

In this work, we synthesized a phosphotungstic acid co-doped with silver and ammonium ions and tested its catalytic activity in the liquid-phase esterification of oleic acid and methanol for biodiesel production. The effect of various process parameters on the esterification reaction was investigated to optimize the efficiency of this system for biodiesel production. Moreover, the reusability of the catalyst and additional experiments for the catalytic esterification of other free fatty acids and non-edible oils with methanol were also studied.

2. Experimental

2.1. Materials

Phosphotungstic acid (AR), silver nitrate (AR), ammonium carbonate (AR), oleic acid (AR), methanol (AR, >99%), lauric acid (AR, 98%), stearic acid (AR, 98%), myristic acid (AR, 98%), palmitic acid (AR, 98%) and methanol (AR, >99%) were purchased from Sinopharm Chemical Regent Co., Ltd. All other chemicals were of analytical grade and used as received, unless otherwise noted.

2.2. Materials preparation and characterization

The ammonium and silver co-doped phosphotungstic acid was prepared according to previous literature[21,22] with slight modifications. In a typical procedure, phosphotungstic acid ($H_3PW_{12}O_{40}$, HPW, 2.88 g, 0.2 mol L^{-1}) was dissolved in deionized water with vigorous stirring at room temperature, and then an ammonium carbonate aqueous solution (0.2 mol L^{-1}) was added dropwise, followed by the addition of a silver nitrate (0.2 mol L^{-1}) aqueous solution, and was kept under stirring conditions for over 1 h at room temperature. The obtained mixture was heated at 70 °C for 3 h, and finally dried under vacuum at 110 °C for 12 h to obtain the final co-doped phosphotungstate ($Ag_1(NH_4)_2PW_{12}O_{40}$) catalyst, which was denoted as AgN-PW. The XRD patterns of the catalysts were obtained using a Rigaku D/max 2000 ultima plus diffractometer (monochromatic nickel filter, Cu Kα radiation). The FT-IR spectra were scanned on a PerkinElmer spectrum100 using the KBr disc technique (4000–400 cm^{-1}). Thermogravimetric analysis (TGA) was performed on a NETZSCH/STA 409 PC Luxx simultaneous thermal analyzer with a heating rate of 5 °C min^{-1} under an air flow rate of 20 mL min^{-1}. The BET surface area, total pore volume and pore size distribution of the catalyst were determined with a Micromeritics ASAP 2020 V4.02 volumetric adsorption analyzer. Scanning electron microscopy (SEM) images were obtained on a JEOL-6701F scanning electron microscope at 10.0 kV. Transmission electron microscopy (TEM) was carried out on a JEOL 2100F electron microscope operated at 200 kV.

2.3. The esterification test

The esterification test was carried out as follows. In a typical procedure, certain amounts of oleic acid, methanol and catalyst were mixed and heated at 70 °C for 4.0 h under vigorous stirring. Upon completion, the catalytic system was cooled down to room temperature immediately, and the catalyst was separated from the reaction mixture by filtration, and purified under reduced pressure to remove excess methanol. The acid value (AV, mg KOH g^{-1}) and the conversion rates could be calculated using the following formulas, by referring to the ISO 660-2009 standard.[23,24] The reaction parameters *i.e.* the amount of catalysts, the molar ratio of oleic acid to methanol, the reaction time and temperature were regulated within a certain range to optimize the conversion of oleic acid.

$$\mathrm{AV} = \frac{V_{\mathrm{KOH}} \times C_{\mathrm{KOH}} \times 56.1}{\text{weight of sample}} \quad (1)$$

$$\text{Conversion } (\%) = \frac{\mathrm{AV}_1 - \mathrm{AV}_2}{\mathrm{AV}_1} \times 100\% \quad (2)$$

3. Results and discussion

3.1. Characterization

3.1.1. XRD analysis of the catalyst. The XRD patterns of the prepared mesoporous AgN-PW catalyst and those of the pristine HPW are presented in Fig. 1. Pristine HPW showed seven main diffraction peaks approximately at 2θ values of 9.1°, 20.3°, 25.8°, 27.5°, 28.7°, 31.6° and 35.9°, which can be attributed to the characteristic peaks of the body-centered cubic secondary structure of the Keggin anion.[24] In the case of the silver and ammonium ion substituted HPW catalyst, the same diffraction patterns were observed with a marginal shift towards higher 2θ values (10.6°, 21.3°, 26.2° and 30.4°) indicating a contracted unit cell.[25,26]

3.1.2. FT-IR analysis of the catalyst. The FT-IR spectra of pristine HPW and the synthesized AgN-PW are presented in Fig. 2. The spectrum of pristine HPW showed the characteristic Keggin structure with bands at 1080 cm^{-1}, 982 cm^{-1}, 889 cm^{-1}

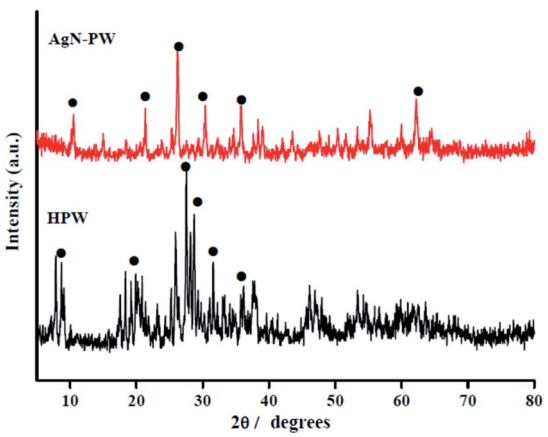

Fig. 1 XRD patterns of pristine HPW and AgN-PW catalysts.

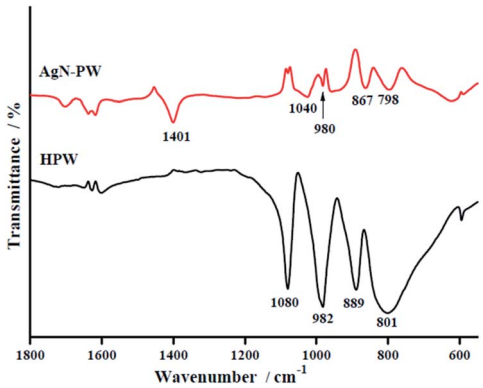

Fig. 2 FT-IR spectra of the pristine HPW and the AgN-PW catalyst.

and 801 cm^{-1}, corresponding to the stretching vibration of P–O in the central PO_4 tetrahedron, the terminal bonds of W–O in the exterior, the W–O_b–W bridge between corner sharing octahedra, and the W–O_c–W bridges between edge sharing octahedra, respectively,[27,28] and the pristine HPW can be detected from the Keggin anion in the structure. These characteristic bands (1040 cm^{-1}, 980 cm^{-1}, 867 cm^{-1} and 798 cm^{-1}) were also found in the spectra of ammonium and silver ion substituted HPW, indicating that the Keggin structure was maintained in the AgN-PW catalyst, and the red shift was caused by the replacement of larger Ag^+ and NH_4^+ ions for smaller H^+. In addition, there was also a band related to N–H stretching observed at 1401 cm^{-1}, indicating that the ammonium ion was successfully exchanged for hydrogen in the HPW.[22]

3.1.3. TG analysis of the catalyst. The thermal stability of the AgN-PW catalyst was investigated by thermogravimetric (TG) analysis as shown in Fig. 3. The first mass loss of 2.8% (between 40 and 270 °C) may be due to the removal of surface-adsorbed water from the catalyst; and the second mass loss of 2.7% (between 300 and 600 °C) can be ascribed to the separation of NH_3 molecules from AgN-PW.[29] The dissociation of NH_4^+ in the high-temperature region indicated that the replacement of H^+ with metal ions in HPW can enhance its thermal stability, which is consistent with reports in the literature.[21,30] Accordingly, the AgN-PW sample will be a desirable catalyst in the esterification reaction of biodiesel production with its high thermal stability.

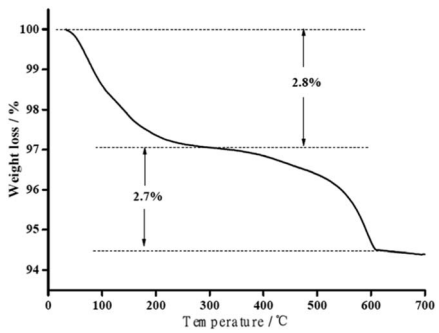

Fig. 3 TG analysis of the AgN-PW catalyst.

3.1.4. Nitrogen adsorption–desorption of the catalyst. Nitrogen adsorption–desorption isotherms for the AgN-PW catalyst are illustrated in Fig. 4. The catalyst displayed representative type IV curves, and the hysteresis loop at the P/P_0 value of 0.35–1.0 indicated typical mesoporous structures, which are characteristic of solids formed from aggregates with uniform pore size and large channel-like mesopores with a narrow pore size distribution.[31,32]

3.1.5. SEM and TEM analysis of the catalyst. Further information about the surface morphology of the pristine HPW and the AgN-PW catalysts was obtained from the SEM micrographs as presented in Fig. 5. The pristine HPW (Fig. 5a) shows large agglomerates with an irregular block structure, however, the morphology of the AgN-PW sample (Fig. 5b) shows nanospheres with a mean size of 500–600 nm, indicating a successful exchange of the hydrogen ions for the ammonium and silver ions. For AgN-PW, a mesoporous structure was observed in the TEM image (Fig. 5c), which was consistent with the nitrogen adsorption–desorption data.

3.2. Catalytic activity of the mesoporous AgN-PW for esterification

3.2.1. Effect of the reaction time. The esterification reaction of oleic acid was performed for the mesoporous AgN-PW catalyst for different durations ranging from 1.0 h to 7.0 h to study the effect of the reaction time on the conversion. Other reaction parameters which remained constant were as follows: an oleic acid to methanol molar ratio of 1 : 10, a catalyst loading of 250 mg and a reaction temperature of 70 °C. As shown in Fig. 6a, a sufficient reaction time (1.0 h to 4.0 h) was crucial to obtain a high conversion in the esterification. However, as the reaction time was prolonged to 4.0 h, there was no significant increase in the conversion. This was probably due to the esterification being reversible, which easily took place when the reaction time lasted more than 4.0 h.[33] This result indicated that the optimum reaction time for the catalyst was 4.0 h.

3.2.2. Effect of the catalyst amount. To study the effect of catalyst amount on the reaction, the reaction was performed with different amounts of catalyst (0, 50, 100, 150, 200, 250, 300, 350 mg) under the condition of an oleic acid/methanol ratio of

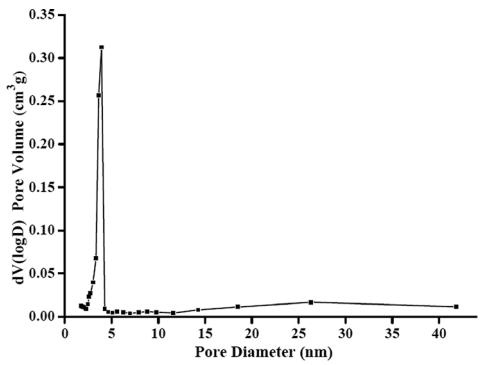

Fig. 4 N_2 adsorption–desorption isotherms and pore size distribution (in the inset) of the AgN-PW catalyst.

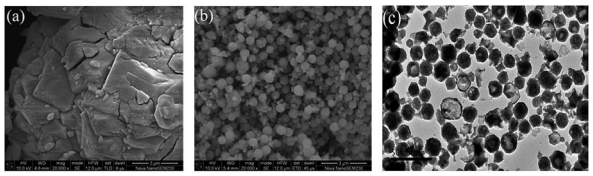

Fig. 5 SEM images of the pristine HPW (a) and the AgN-PW (b), and TEM image of the AgN-PW (c).

1 : 10 for 4 h at 70 °C. As shown in Fig. 6b, the conversion rate significantly increased with the amount of catalyst from 50 mg to 250 mg. The biodiesel conversion reached 96.1% with a catalyst amount of 250 mg, this result was due to an increase in the amount of available catalytic active sites as the amount of catalyst increased. However, the conversion rate decreased when the catalyst amount was increased to above 300 mg, and this phenomenon can be explained because the excess catalyst amount made the slurry viscous on account of the emulsification and more products were adsorbed.[34,35] Therefore, 250 mg was chosen as the optimum catalyst amount and was used for further investigation in the present research.

3.2.3. Effect of the reaction temperature. The influence of the reaction temperature on the oleic acid conversion was investigated at different temperatures ranging from 20 °C to 70 °C when using mesoporous AgN-PW as the catalyst for 4 h with a catalyst amount of 250 mg and an oleic acid to methanol molar ratio of 1 : 10. As shown in Fig. 6c, the oleic acid conversion increased from 32.3% at 20 °C to 96.1% at 70 °C, and higher temperatures may lead to lower yields because of more evaporation of methanol.[36] In conclusion, the optimum temperature was approximated to 70 °C.

3.2.4. Effect of the oleic acid-to-methanol molar ratio. The impact of the molar ratio of oleic acid to methanol on the esterification process catalyzed by the mesoporous AgN-PW catalyst (70 °C, 4 h) is shown in Fig. 6d. Decreasing the oleic acid to methanol molar ratio from 1 : 2 to 1 : 10 can result in a remarkable increase in oleic acid conversion. However, lower ratios (*e.g.* 1 : 14 and 1 : 18) were found to negatively influence the conversion. Previous studies have suggested that this phenomenon could possibly be attributed to insufficient mixing of the reactants and products with the solid acid catalyst, as well as the decrease in catalyst concentration.[37,38] Therefore, the optimum oleic acid to methanol molar ratio for this system was 1 : 10.

3.3. Catalyst reusability

Compared with homogeneous inorganic acids, solid acids were a better choice with the advantages of easy separation and good reusability.[39] In this case, the mesoporous AgN-PW sample exhibited desirable oleic acid conversion (56.0%) after four successive cycles under the above-mentioned optimal conditions (see Fig. S1†). The observed decline may be due to the blockage of some active sites by residual adsorbed intermediates and products in spite of the sufficient extraction. The

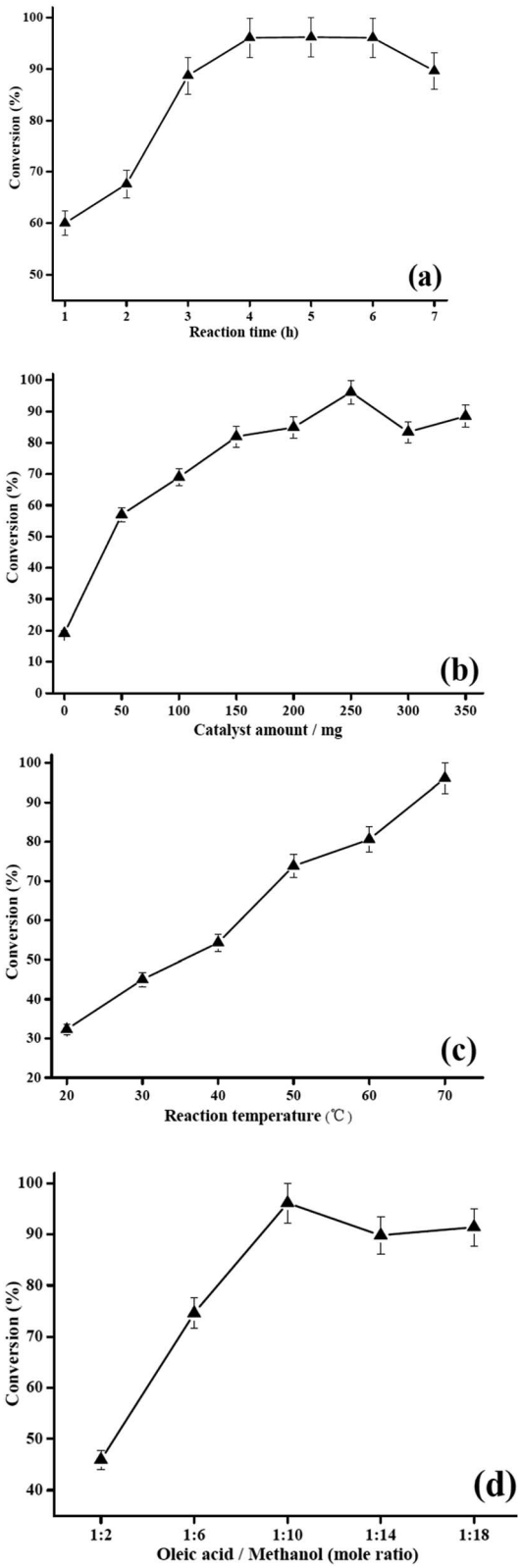

Fig. 6 Effects of time (a), catalyst amount (b), temperature (c) and molar ratio (d) on the oleic acid esterification conversion.

indistinctive FT-IR spectra of fresh AgN-PW and the reused catalyst proved that the Keggin structure was not damaged during the esterification of oleic acid and methanol (see

Fig. S2†). These results demonstrate the good stability of the AgN-PW composite.

3.4. Catalytic performance of AgN-PW for other esterifications

In order to extend the scope of the mesoporous AgN-PW catalyst in biodiesel production, further studies of other FFAs with methanol were investigated (see Table S1†). When lauric acid, myristic acid, palmitic acid, stearic acid and non-edible oils were subjected to the esterification reaction with methanol, high FFA conversions were obtained as well, *e.g.* 76.0% of stearic acid and 90.7% of non-edible oils, superior to those of other reports.[40] These results show that the mesoporous AgN-PW catalyst has great potential to catalyze many types of esterification reactions to meet the demand of synthetic biodiesel.

4. Conclusions

In summary, we described a facile synthesis strategy of a mesoporous silver and ammonium co-doped phosphotungstate material with a Keggin structure. This material displayed excellent catalytic performance with an oleic acid conversion of 96.1% in the esterification, under the following optimal conditions: 250 mg of catalyst, a molar ratio of 1 : 10 of oleic acid to methanol, a reaction time of 4.0 h and a reaction temperature of 70 °C. This sample displayed good catalytic performance in other FFA esterifications, such as lauric acid, myristic acid, palmitic acid and stearic acid esterification. Moreover, this catalyst could be reused and was stable for a few cycles. Therefore, the mesoporous AgN-PW sample could be a promising catalyst in industrial biodiesel production.

Conflicts of interest

There are no conflicts to declare.

Acknowledgements

This work was financially supported by the youth growth S&T personnel foundation of the Guizhou education department (KY [2016]272), the Joint Science and Technology Funds of the Guizhou S&T department, the Anshun city people's government and Anshun university (LH[2016]7269 and LH[2016]7278), the creative research groups support program of Guizhou education department (No. KY [2017]049), and the 2017 innovative entrepreneurship training program for undergraduates of the Guizhou education department (201710667025).

Notes and references

1 S. Chu and A. Majumdar, *Nature*, 2012, **488**, 294–303.
2 Q. Y. Zhang, F. F. Wei, D. Luo, P. H. Ma and Y. T. Zhang, *China Pet. Process. Petrochem. Technol.*, 2017, **19**, 26–32.
3 F. Zhang, X. F. Tian, M. Shah and W. J. Yang, *RSC Adv.*, 2017, **7**, 11403–11413.
4 A. W. Go, S. Sutanto, L. K. Ong, P. L. Tran-Nguyen, S. Ismadji and Y. H. Ju, *Renewable Sustainable Energy Rev.*, 2016, **60**, 284–305.
5 Q. Y. Zhang, H. Li, X. F. Liu, W. T. Qin, Y. P. Zhang, W. Xue and S. Yang, *Energy Technol.*, 2013, **1**, 735–742.
6 Rozina, S. Asif, M. Ahmad, M. Zafar and N. Ali, *Renewable Sustainable Energy Rev.*, 2017, **74**, 687–702.
7 Q. Y. Zhang, F. F. Wei, P. H. Ma, Y. T. Zhang, F. H. Wei and H. L. Chen, *Waste Biomass Valorization*, 2017, DOI: 10.1007/s12649-017-9865-5.
8 C. Muthukumaran, R. Praniesh, P. Navamani, R. Swathi, G. Sharmila and N. M. Kumar, *Fuel*, 2017, **195**, 217–225.
9 J. Sáez-Bastante, C. Ortega-Román, S. Pinzi, F. R. Lara-Raya, D. E. Leiva-Candia and M. P. Dorado, *Bioresour. Technol.*, 2015, **185**, 116–124.
10 N. Shibasaki-Kitakawa, K. Hiromori, T. Ihara, K. Nakashima and T. Yonemoto, *Fuel*, 2015, **139**, 11–17.
11 R. Z. Raia, L. S. D. Silva, S. M. P. Marcucci and P. A. Arroyo, *Catal. Today*, 2017, **289**, 105–114.
12 A. F. Lee and K. Wilson, *Catal. Today*, 2015, **242**, 3–18.
13 S. W. Gong, L. Jing, H. H. Wang, L. J. Liu and Q. Zhang, *Appl. Energy*, 2014, **134**, 283–289.
14 R. Purova, K. Narasimharao, N. S. I. Ahmed, S. Al-Thabaiti, A. Al-Shehri, M. Mokhtar and W. Schwieger, *J. Mol. Catal. A: Chem.*, 2015, **406**, 159–167.
15 S. Jeenpadiphat, E. M. Björk, M. Odén and D. N. Tungasmita, *J. Mol. Catal. A: Chem.*, 2015, **410**, 253–259.
16 K. Saravanan, B. Tyagi, R. S. Shukla and H. C. Bajaj, *Fuel*, 2016, **165**, 298–305.
17 T. M. M. Marso, C. S. Kalpage and M. Y. Udugala-Ganehenege, *Fuel*, 2017, **199**, 47–64.
18 F. N. D. C. Gomes, F. M. T. Mendes and M. M. V. M. Souza, *Catal. Today*, 2017, **279**, 296–304.
19 M. Safariamin, S. Paul, K. Moonen, D. Ulrichts, F. Dumeignil and B. Katryniok, *Catal. Sci. Technol.*, 2016, **6**, 2129–2135.
20 K. Narasimharao, D. R. Brown, A. F. Lee, A. D. Newman, P. F. Siril, S. J. Tavener and K. Wilson, *J. Catal.*, 2007, **248**, 226–234.
21 J. S. Santos, J. A. Dias, S. C. L. Dias, J. L. de Macedo, F. A. C. Garcia, L. S. Almeida and E. N. C. B. de Carvalho, *Appl. Catal., A*, 2012, **443–444**, 33–39.
22 X. Zhou, Z. X. Li, C. Zhang, X. P. Gao, Y. Z. Dai and G. Y. Wang, *J. Mol. Catal. A: Chem.*, 2016, **417**, 71–75.
23 A. M. Doyle, T. M. Albayati, A. S. Abbas and Z. T. Alismaeel, *Renewable Energy*, 2016, **97**, 19–23.
24 G. Raveendra, A. Rajasekhar, M. Srinivas, P. S. Sai Prasad and N. Lingaiah, *Appl. Catal., A*, 2016, **520**, 105–113.
25 S. H. Zhu, X. Q. Gao, F. Dong, Y. L. Zhu, H. Y. Zheng and Y. W. Li, *J. Catal.*, 2013, **306**, 155–163.
26 Y. S. Ren, B. Liu, Z. H. Zhang and J. T. Lin, *J. Ind. Eng. Chem.*, 2015, **21**, 1127–1131.
27 M. Nyman, F. Bonhomme, T. M. Alam, J. B. Parise and G. M. B. Vaughan, *Angew. Chem., Int. Ed.*, 2004, **43**, 2787–2792.
28 D. Y. Zhang, M. H. Duan, X. H. Yao, Y. J. Fu and Y. G. Zu, *Fuel*, 2016, **172**, 293–300.

29 A. B. Gawade, M. S. Tiwari and G. D. Yadav, *ACS Sustainable Chem. Eng.*, 2016, **4**, 4113–4123.
30 S. K. Bhorodwaj and D. K. Dutta, *Appl. Catal., A*, 2010, **378**, 221–226.
31 K. Wang, L. Yang, W. Zhao, L. Q. Cao, Z. L. Sun and F. Zhang, *Green Chem.*, 2017, **19**, 1949–1957.
32 R. Dutta, S. K. Singh, S. A. Mandavgane and J. D. Ekhe, *Appl. Catal., A*, 2017, **539**, 38–47.
33 H. Pan, H. Li, X. F. Liu, H. Zhang, K. L. Yang, S. Huang and S. Yang, *Fuel Process. Technol.*, 2016, **150**, 50–57.
34 G. Baskar and S. Soumiya, *Renewable Energy*, 2016, **98**, 101–107.
35 Q. Y. Zhang, F. F. Wei, Y. T. Zhang, F. H. Wei, P. H. Ma, W. Zheng, Y. T. Zhao and H. L. Chen, *J. Oleo Sci.*, 2017, **66**, 491–497.
36 Y. L. Liu, P. B. Zhang, M. M. Fan and P. P. Jiang, *Fuel*, 2016, **164**, 314–321.
37 B. Freedman, E. H. Pryde and T. L. Mounts, *J. Am. Oil Chem. Soc.*, 1984, **61**, 1638–1643.
38 S. Chaveanghong, S. M. Smith, C. Oopathum, C. B. Smith and A. Luengnaruemitchai, *Renewable Energy*, 2017, **109**, 480–486.
39 Y. Zhou, S. L. Niu and J. Li, *Energy Convers. Manage.*, 2016, **114**, 188–196.
40 M. A. R. Melo Júnior, C. E. Albuquerque, J. S. A. Carneiro, C. Dariva, M. Fortuny, A. F. Santo, S. M. S. Egues and A. L. D. Ramos, *Ind. Eng. Chem. Res.*, 2010, **49**, 12135–12139.